Available online at www.rajournals.in

RA JOURNAL OF APPLIED RESEARCH
ISSN: 2394-6709
DOI:10.31142/rajar/v4i5.02
Volume: 04 Issue: 05 May -2018

International Open Access
ICV- 74.25
Page no.- 1666-1683

Dynamic Modeling, and Simulation of Hybrid Solar Photovoltaic, and PEMFC Fuel Cell Power System

S. Sami [1,2] , E. Marin[2]

[1,2]Research Center for Renewable Energy Catholic University of Cuenca, Cuenca, Ecuador
[1]TransPacific Energy, Inc, NV 89183 US

ARTICLE INFO

Published Online:
06 May 2018

Corresponding author
S. Sami

ABSTRACT

The dynamic energy conversion equations have been developed to describe the behavior of a hybrid system of solar photovoltaic, and fuel cell as well as hydrogen storage. The system of equations has been integrated, and solved simultaneously using finite difference formulation. The dynamic model is intended for optimization and design purposes. On-site data was used to validate the simulation program under various conditions. Comparison between the data and predicted results showed a fair agreement.

KEYWORDS: Modeling, Simulation, Hybrid System, Photovoltaic, Fuel Cell, Hydrogen Storage, Experimental Validation

Introduction:

Renewable and nonconventional methods of power such as hybrid systems offer supply solutions for remote areas, not accessible by grid power supply and in use of distributed generation [1]. Integrated system of two or more renewable energy systems, also known as hybrid renewable energy system, is becoming popular because these sources can complement each other, provide higher quality and more reliable power supply independent of the grid and electrify rural areas [2-4]. Of a particular interest is the electrification of rural area and power standalone systems that have been presented and discussed by reference [5-7].

On the other hand, the modeling and simulation of solar-photovoltaic, wind and fuel cell hybrid energy systems using MATLAB/Simulink software were reported and the simulation results the hybrid systems were also presented and discussed by Mahallakshmi, and Latha [7]. Maharia and Dalal [8] reported on hybrid photovoltaic-fuel cell generating system designed for remote areas or isolated loads and an electrolyzer for hydrogen generation and storage was also reported. In addition, the system included a controller designed to achieve permanent power supply to a load via PV array or a fuel cell or both. Another study by Kumar and Garg [9] dealt with a detailed hybrid model of a solar/ wind and fuel cell in Simulink. They developed a high efficient model and compared with a hybrid model using battery as a storage system instead of fuel cell. Furthermore, another potential solution for stand-alone power generation for remote areas was presented by Touati et al. [10] for a hybrid energy system in parallel with some hydrogen energy storage. In this study the hybrid PV, fuel cell generation employed an electrolyzer using reverse osmosis driven by PV for hydrogen generation that is applicable to desalination plant loads. Furthermore, Hieu Nguyen [11] presented a mathematical model to predict the behavior of PV system for sizing and simulation of PV. Modeling and sizing of hybrid systems that includes PV was presented that are based upon the daily source data were calculated using monthly mean solar radiation. References [12-23] discussed a design of a hybrid power system for PV, wind turbine and battery connected to the grid.

This paper presents a numerical modeling of the dynamic behavior of a hybrid solar photovoltaic, and fuel cell power system for either on or off the grid applications. This particular hybrid power generation system is of a particular interest since the fuel cell is driven in part of electricity generated by the solar photovoltaic. The end result is a more efficient energy conversion as well as power generation for either off the grid or on the grid. The model presented hereby uses the conversion energy equations and finite difference formulations to describe the dynamic behavior of the hybrid system.

This paper also describes the simulation, of the fuel cell/hydrogen storage system that can be used during low solar radiation. The following describes the simulation model, energy conversion equations, as well as energy conversion efficiencies

Mathematical Modeling:

In the following sections, the energy conversion equations and finite difference formulations for each source of renewable energy are presented;

Photovoltaic PV system:

The thermal energy absorbed by the PV solar collector is [1, 3];

$$P_{pv} = \eta_{pvg} A_{pvg} G_t \quad (1)$$

Where η_{pvg} is PV solar collector efficiency, A_{pvg} is PV solar collector area (m^2), and G_t is solar irradiation (W/m^2) and η_{pvg} can be defined as [1];

$$\eta_{pvg} = \eta_r \eta_{pc}[1 - \beta(T_c - T_{c\,ref})] \quad (2)$$

Where η_{pc} is power conditioning efficiency which is equal to one when maximum power point tracking (MPPT) is used, and β is temperature coefficient ((0.004 – 0.006) per °C), and η_r is the reference module efficiency, and $T_{c\,ref}$ is the collector reference temperature.

The Photovoltaic output current can be determined from the following equation [11, 26];

$$I = N_p * I_{ph} - N_p * I_o * \left[\exp\left(\frac{\frac{U}{N_s} + I * \frac{R_s}{N_p}}{n * V_t}\right) - 1\right] - I_{sh} \quad (3)$$

Where;

N_p = Total number of cells in parallel
N_s = Total number of cells in series
I_{ph} = Photovoltaic module (A)
I_o = Saturation current of the module
V_t = Diode thermal voltage
U = Voltage (V)

The photovoltaic module current is determined from the following equation [11-16];

$$I_{ph} = [I_{sc} + K_i(T - 298)] * \frac{I_r}{1000} \quad (4)$$

Where;

I_{sc} = Short-circuit current (A)
K_i = Short-circuit current of the cell at 25 ° C and 1000 W / m²
T = Operating temperature (K)
I_r = Solar irradiation (W/m²)

The reverse saturation current of the module is determined from [11-16];

$$I_{rs} = \frac{I_{sc}}{\left[\exp\left(\frac{qV_{oc}}{N_s K_n T}\right) - 1\right]} \quad (5)$$

Where;

I_{sc} = Short-circuit current (A)
q = Electron Load (C)
V_{oc} = Open Circuit Voltage (V)
n = diode ideality factor
k = Boltzmann constant (J/K)
T = Temperature (K)

Whereas, the saturation current of the module is given by;

$$I_o = I_{rs}\left[\frac{T}{T_r}\right]^3 \exp\left[\frac{q * E_{g0}}{nk}\left(\frac{1}{T} - \frac{1}{T_r}\right)\right] \quad (6)$$

Where;

I_{rs} = Reverse saturation current of the module
T = Temperature (K)
T_r = Rated temperature (K)
q = Electron Load (C)
E_{g0} = Semiconductor energy separation band (eV)

And the shunt resistance current is;

$$I_{sh} = \frac{V * \frac{N_p}{N_s} + I * R_s}{R_{sh}} \quad (7)$$

V = Voltage (V)
I = Current (A)
R_s = Series resistance (Ω)
R_{sh} = shunt resistance (Ω)

Fuel cell model:

The fuel cell output voltage can be obtained as follows [18-23];

$$U_S = U_{th} - U_{act} - U_{ohm} - U_{conc} \quad (8)$$

U_{th} = Theoretical voltage
U_{act} = Charge Transfer Voltage
U_{ohm} = Resistance or ohm voltage
U_{conc} = Voltage of Concentration

The reversible cell tension is calculated after [19];

$$U_{th} = 1{,}2297 + (T - 298{,}15)\frac{\Delta S_o}{nF} + \frac{RT}{nF}\ln\left(\frac{P_{h_2} * P_{o2}^{1/2}}{P_{o}^{1/3}}\right) \quad (9)$$

ΔS_o = Reaction entropy change of liquid water under standard test conditions (KJ / k / mol)
n = Number of electrons per mole
F = Faraday constant (C/mol)
R = Universal gas constant
T = Cell operating temperature

The Charge Transfer Voltage is;

$$U_{act} = \frac{dV_{act}}{dt} = \frac{I_s}{C} - \frac{U_{act}}{\frac{R_a}{C}} \quad (10)$$

The transient voltage in equation (14) can be obtained as follows [19];

$\frac{dV_{act}}{dt}$ = Transient voltage (V)
I_s = Current (A)
C = Constant (108.75 F)
R_a = Activation resistance

And;

$$R_a = \frac{-\eta_{act}}{I_s} \quad (11)$$

The activation voltage is also calculated after the following equation [19];

$$\eta_{act} = 0{,}9514 + 0{,}00312\,T - 0{,}000187\,T\,\ln(i) + 7{,}4x10^{-5}\,T\ln(C_{o2}) \quad (12)$$

Where;

η_{act} = Activation voltage drop
I_s = Current (A)
T = Temperature
i = Current (A)
C_{o2} = Dissolved Oxygen Concentration

Where;

$$C_{o2} = \frac{P_{o2}}{5{,}08x10^6 \exp\left(\frac{-498}{T}\right)} \quad (13)$$

P_{o2} = Oxygen pressure on the cathode side
T = Temperature
The fuel cell load is obtained as [10];

$$E_{H2} = \frac{Load}{\eta_{FC}} \quad (14)$$

E_{H2} = Amount of Energy
$Load$ = Maximum and minimum amount of energy storage in KWh
η_{FC} = Fuel Cell Efficiency
The hydrogen mass is [10];

$$m_{H2} = \frac{E_{H2}}{PCS_{H2}} \quad (15)$$

Where;
m_{H2} = Hydrogen mass
E_{H2} = Amount of Energy
PCS_{H2} = Higher calorific value of H2
Since the hydrogen density is equal 0.085 kg/m^3, then the hydrogen's volume can be calculated as follows;

$$V_{H2} = \frac{m_{H2}}{0.085} \quad (16)$$

V_{H2} = Volume of hydrogen
m_{H2} = Hydrogen mass
The compressor power to store the hydrogen at higher pressure is [10];

$$P_{comp} = \frac{q_{gas} T_e C_p}{\eta_C}\left(\left(\frac{P_s}{P_e}\right)^{\frac{\gamma-1}{\gamma}} - 1\right) \quad (17)$$

P_{comp} = Compression Power
q_{gas} = Gas Mass Flow Rate (kg/s)
T_e = Gas Inlet Temperature (k)
C_p = Calorific amount of gas (J/kg.k)
η_C = Compressor Output
P_s = Compressor Output pressure (atm)
P_e = Compressor Inlet Pressure (atm)
γ = Isentropic coefficient of gas
Finally, the work required for compressing the hydrogen is [10];

$$E_{comp} = Mass * \frac{\gamma-1}{\gamma}\frac{P_e V_o}{\eta_C}\left(\left(\frac{P_s}{P_e}\right)^{\frac{\gamma-1}{\gamma}} - 1\right) \quad (18)$$

E_{comp} = Compression energy
$Mass$ = mass of hydrogen

Electrolyzer:

The electrolyzer is driven by part of the solar photovoltaic panels output to produce hydrogen. Each electrode has a single polarity producing either H_2 or O_2. The operating temperature of the electrolyzer does not exceed 70 °C. This model considers the Proton Exchange Membrane Fuel Cell (PEMFC). The hydrogen production rate is given by [10, and 27];

$X_H = 5.18 \times e^{-6} I_e$ (mole/s) (19)

Where I_e is the current between electrodes, it is assumed that the H_2 is stored in a tank normally under 3 bars and feeds then fuel cell.

The electric fuel cell power output in DC can be expressed as following;

$$P_{FC}(t) = \eta_{c3} I_{FC}(t).V_{FC}(t) \quad (20)$$

Controller:

Generally, the controller power output is given by;

$$P_{Cont-dc} = V_{bat}(I_{rect} + I_{PV} + I_{FC}) \quad (21)$$

Where; V_{bat} is multiplication of the nominal voltage DC in the battery for any particular system and I_{rect}, I_{PV} and I_{FC} represent the output current of the rectifier in DC and currents of PV and fuel cell.

Battery Performance Model:

Normally, batteries in a hybrid system are connected in series to obtain the appropriate nominal bus voltage. Therefore, the number of batteries connected in series in a battery banks is calculated as follows;

$$N_{SBat} = \frac{V_{PV}}{V_{Bat}} \quad (22)$$

Where, V_{pv} and V_{bat} are the PV and battery voltage, respectively.

Inverter, Charger, and Loads Performance Model:

The characteristics of the inverter are given by the ratio of the input power to the inverter P_{inv-ip} and inverter output powerP_{inv-op}. The inverter will incur conversion losses and to account for the inverter efficiency losses, η_{inv} is used;

$$P_{inv-ip}.\eta_{inv} = P_{inv-op} \quad (23)$$

In many applications, load may not be served with the desired amount of energy. This situation is described as loss of load probability (LLP) and can be calculated using the following equation and, LLP can represent the system reliability [10, 13, 27];

$$LLP = \frac{Energy\_Demand}{Energy\_Served} \quad (24)$$

The AC power of the inverter output P(t) is calculated using the inverter efficiency η_{inv} , output voltage between phases, neutral V_{fn}, for single-phase current I_o and $cos\varphi$ as follows [27];

$$P(t) = \sqrt{3}\,\eta_{inv} V_{fn} I_o\, cos\varphi \quad (25)$$

The hybrid system energy conversion efficiency for harnessing energy from solar and fuel cell is given by;

$$\eta_{sh} = \frac{P(t)pv + P(t)Fc}{G_{\text{radiation A\_pvg}}} \quad (26)$$

Finally, the electric PV and Fuel cell combined power output in DC taking into account the efficiency of conversion to electric energy is;

$$P_{PV}(t) = \eta_{c2} I_P(t).V_P(t) \quad (27)$$

Where η_{c2} is the conversion efficiency to DC output and $P_P(t)$ refers to the combined PV panel and Fuel Cell output power. The $V_P(t)$ is the combined PV panel and Fuel Cell

voltage and $I_P(t)$ represents the combined PV panel and Fuel Cell outlet amperage as function of time.

Results and Discussion:

In order to solve the aforementioned equation (1) through (27) and taking into account that total power may not be simultaneous, and for validation purposes, this simulation model and the above mentioned equations were integrated, coded and solved using finite difference formulation under various conditions. In the following sections, we present analysis and discussions of the numerical predicted results and validation of the proposed simulation model with experimental data.

The major components of the hybrid system under investigation are shown in Figure 1; photovoltaic, and fuel cell power generation hybrid system generate as well as charge controller and battery. The battery stores excess power going through the load charge controller. The battery keeps voltage within the specified voltage and thus, protects over discharge rates, and prevent overload [27]. To protect the battery against overload, the photovoltaic panel, and the fuel cell power output generator is disconnected from the system when the DC voltage increases above the current level required by the load [27]. To further protect the battery against excessive discharge, the load is disconnected when the DC bus voltage falls below minimum voltage as required by the load when the current is greater than the current generated by the solar panel, and fuel cell. It is quite important to note that the inverter is employed to convert the DC power to AC for AC loads as shown in Figure.1.

Figure .2 displays the numerical iteration solution using finite difference formulation of the simulation model presented in equations (1) through (27) for lumped parameter model and taking into account that total power may not be simultaneous. The numerical calculation procedure starts with the initiation of the independent and dependent parameters and solving the energy conservation and conversion equations (10) through (27), to determine the PV panel output, fuel cell output and the relevant hydrogen storage parameters; mass, hydrogen energy storage, power that can be generated by hydrogen storage as well as the other components. The predicted results are printed once the iteration criteria were reached.

As shown in Figure. 1, the output of the solar panels photovoltaic PV under investigation, is forwarded to the load controller and DC/AC inverter. The output of the load controller is maintained at constant 24 volts, thus the batteries are charged constantly with 24 Volts. With the help with inverter, the output AC voltage is 120 volts depending upon the load. The PV solar two panels array has 240 watt output estimated at irradiance of 1000 w/m^2 with an open circuit current of 15.14 ampere and open circuit volt of 21.7 Volts. The module efficiency and cell temperature are 12.1% and 25 °C respectively. The type of solar cell is mono-crystalline with 156x156 mm. each solar panel has 36 cells and size of the module is 1.482x 0.67x .035 meter.

Figure .3 presents the time variation of solar radiation (W/m2) measured at the site and employed in this simulation. It is quite clear that the intensity of radiation depends upon the hour of the day and the month of the year and even the year. However, average radiation values were only considered in this study.

The solar array output voltage and the amount generated by the solar array of photovoltaic are variable since they depend upon not only on the sun irradiation, and temperatures of the ambient, PV cell temperature and relative humidity.

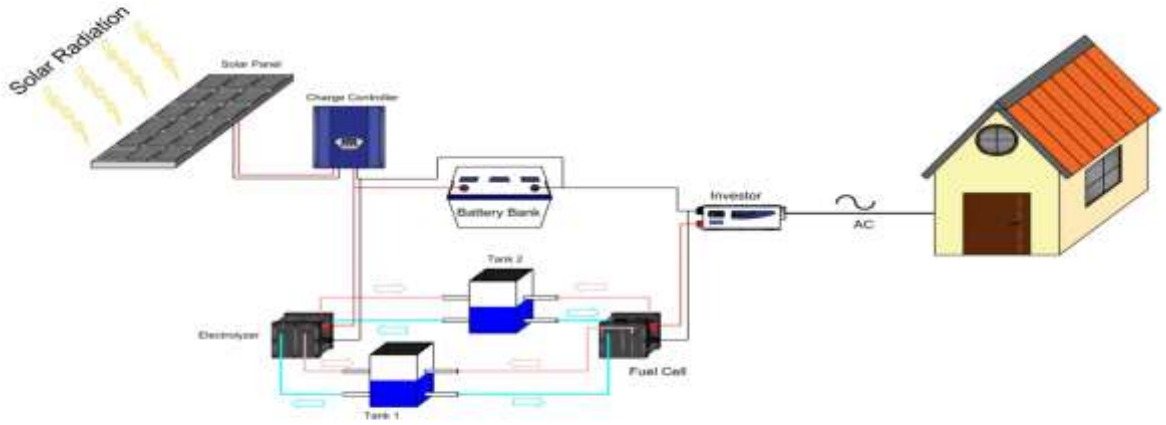

Figure 1. Hybrid Energy System Components.

The load of the hybrid system was shared between the PV solar panels and the fuel cell type PEM with the following ratios; 50/50%, 40/60%, 30/70% by the PV solar panels and the fuel cell, respectively. However, in this study, only the simulation of 50/50% load sharing is presented and discussed hereby in the following sections.

PV solar panel:

The solar PV array output dynamic characteristic depend not only on the sun irradiation, but also on other parameters such as the PV cell temperature and ambient conditions, voltage-current curve as well as the power and voltage which are depicted in Figures 4 through 7 for load shared 50/50 between the PV solar panels and the fuel cell, respectively.

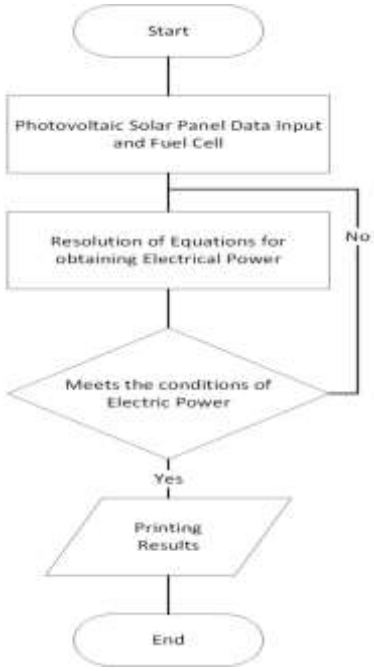

Figure 2. Numerical solution flow chart diagram.

As demonstrated in Figures. 4 through 7, the PV solar characteristics such as cell temperature, amperage and output increases with time, where the solar radiation is converted into electrical energy and increases as time progressed. In addition, similar behavior was observed at different load ratios between the fuel cell and the solar panels. Furthermore, these figures also present the impact of increasing the solar radiation on the PV panel characteristics. It is quite clear from the results in these figures that higher irradiance will result in higher electrical output and energy conversion efficiency. Thus, the solar panels will be more efficient to operate at sites with higher irradiance.

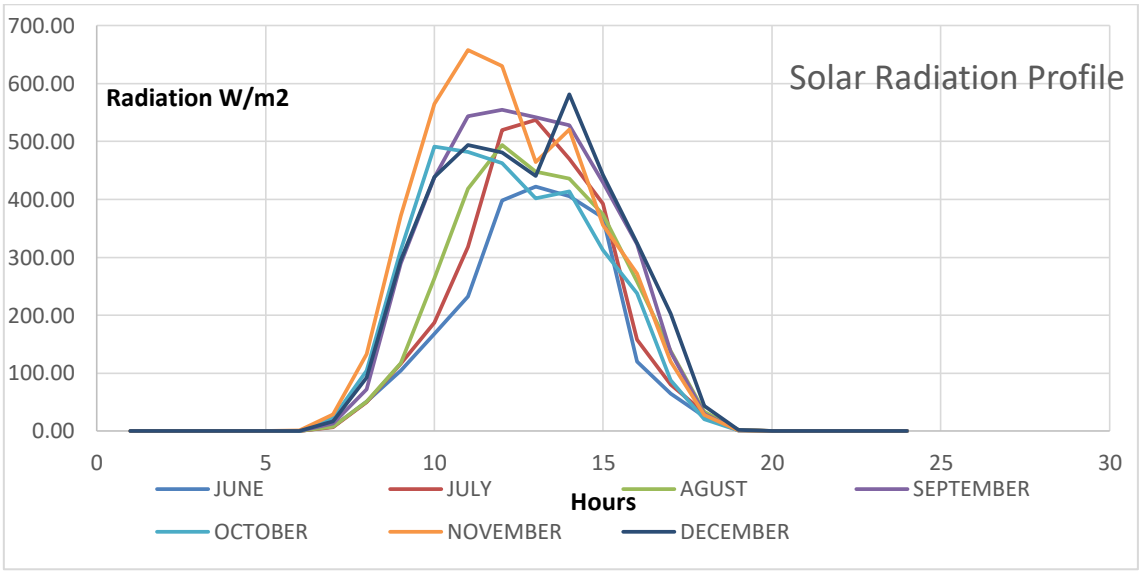

Figure. 3 Time-variation of solar intensity W/m2, 2016.

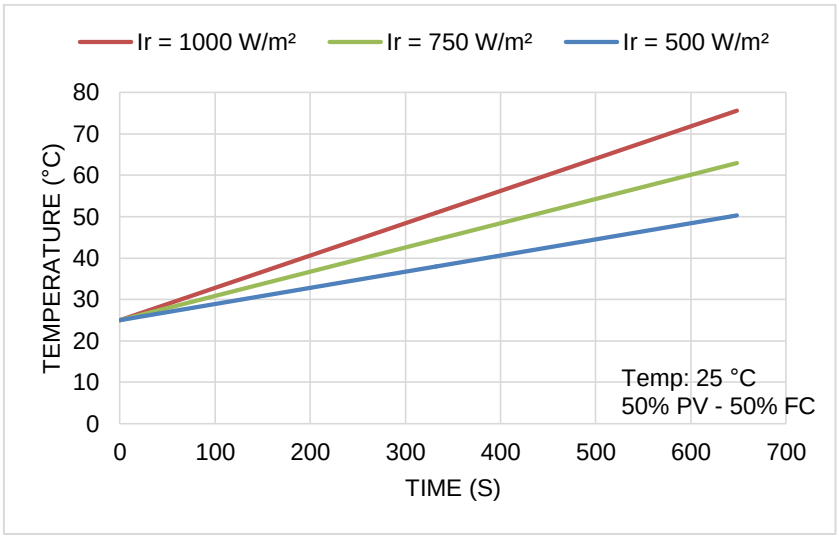

Figure 4: Dynamic PV cell temperature

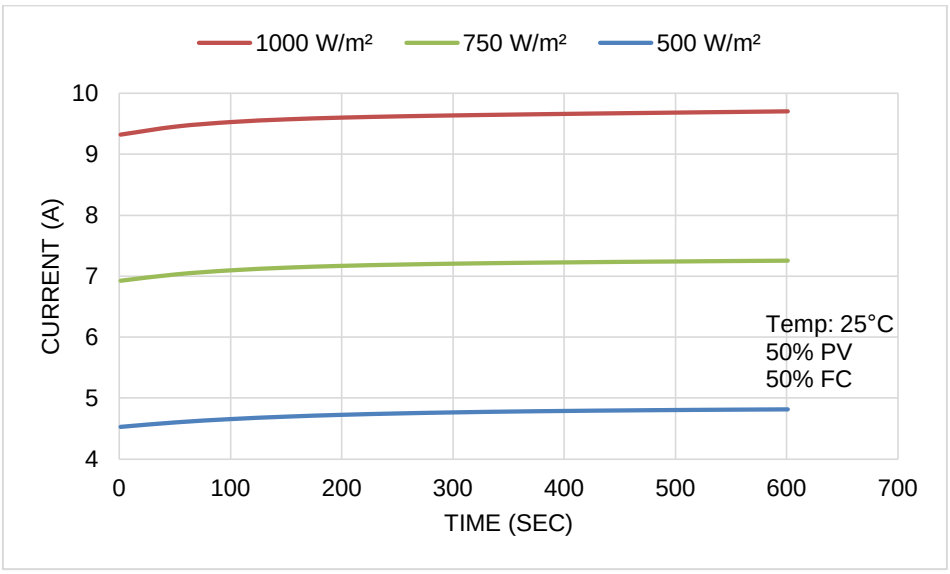

Figure 5: Dynamic PV cell output current

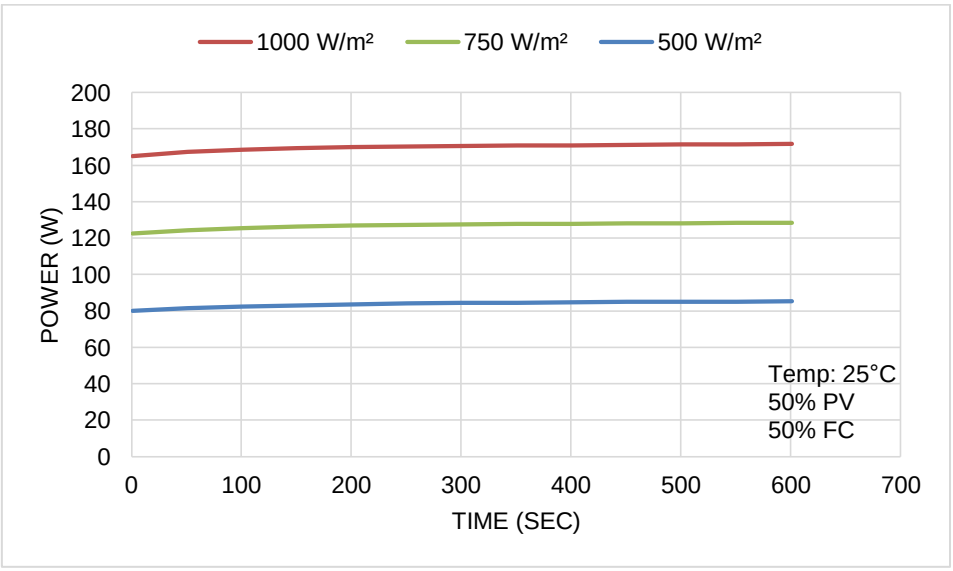

Figure 6: Dynamic PV cell output power

It is also worthwhile to point out that the higher the solar radiation at the site the higher the energy conversion efficiency. Similar observation can be noted at different load sharing between the solar PV and PEM fuel cell as well as in the literature [10, 15, 18].

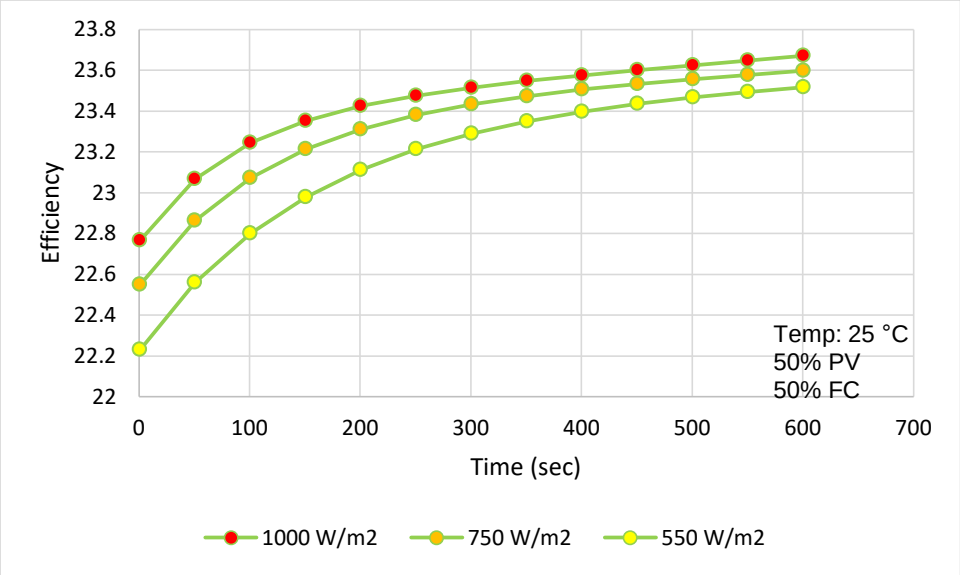

Figure 7: Dynamic PV efficiency at different solar radiation

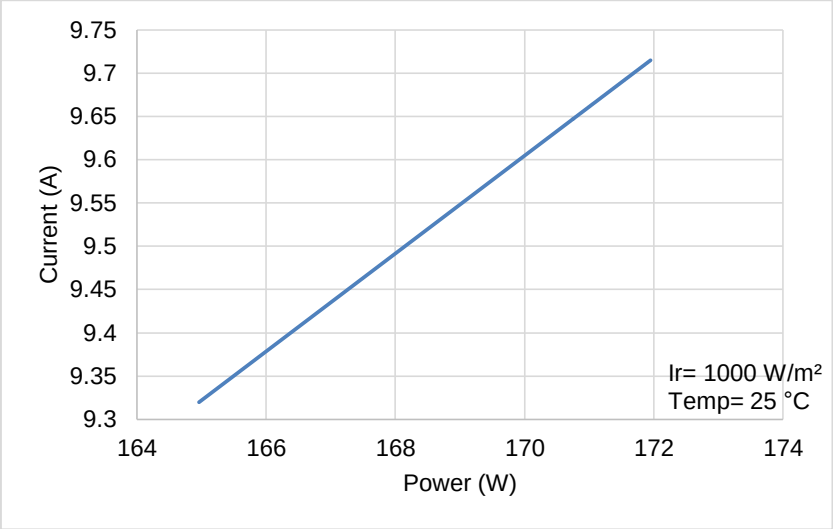

Figure 8: Current- power characteristics of the solar PV panel

On the other hand, Figure. 8 shows the current- power characteristics of the solar PV panes where, higher amperage results in higher power, since the PV solar panel output voltage is kept constant. This relationship has been also observed at other solar radiations for the different load sharing between the solar PV and PEM fuel cell and reported by other references [10,12, 13, 15,18].

PEM Fuel Cell:

A part of the energy provided by the solar panels photovoltaic is used to drive the electrolyzer and result in storing the hydrogen as shown in Figure 1. The electrolyzer is composed of a number of isolated cells from each other in a separate stack. Cell operating voltage at normal conditions is 1.7-1.9 V and the operating temperature does not exceed 70 °C [10]. Polymer Electrolyte Membrane (PEM) fuel cells use hydrogen and oxygen from the air to produce electricity. As shown in Figure 1, the hydrogen leaving the electrolyzer is directed towards the fuel cell. The fuel cell uses hydrogen to produce electricity. The performance of the PEMFC is based upon the voltage produced as the current increases. Theoretically, the ideal voltage of the fuel cell is the Nernst potential, however as indicated in equation (9), with external circuit there are three voltages losses involved in the fuel cell voltage output; activation voltage, ohmic voltage and concentration voltage [7]. The fuel cell under consideration in this study is of type Proton Exchange Membrane Fuel Cell PEMFC [7, 10]. The various terms in equation (9) represents the voltage difference between the cell terminals, and are generated by the movement of electrons through the external circuit and proton through the membrane for a

single cell. This voltage difference was numerically calculated using the theoretical model of a proton exchange membrane (PEM) fuel cell model reported by Najafizadegan and Zarabadipour [17].

Furthermore, Lin et al. [20] presented extremely valuable data used in the numerical model to calculate and validate model as well as the various terms of equation (8) to predict the voltage difference between the cell terminals. It is worthwhile mentioning that the first, second and third terms of equation (8) have functional dependence on the operating temperature of the fuel cell. Furthermore, the fourth term is mainly due to the reactive excess near the catalyst surface and is a function of the current density passing through the cell at each moment.

The fuel cell considered for this simulation, has number of cells; 33, operating temperature; 338 °K, cell active area; 40.6 cm^2 , membrane thickness; 178 µm, current density; 1.42 A/cm^2 and partial pressures of hydrogen and oxygen are 3 atm and 1 atm, respectively. It was also assumed in this simulation model (equations 17 and 18) that η_c =1. γ=1.41, $P_e=10^5$ Pa and V_o = 11.11 m^3/kg of hydrogen.

The dynamic behavior of the fuel cell is presented and discussed in the following sections and in particular in figures 9 through 15. It is quite clear from these figures that the fuel cell behavior during the transient functioning has been enhanced in power depending upon the different key parameters of the fuel cell. In particular, figure .11 showed a noticeable increase in efficiency as the load increases.

Furthermore, the transient behavior is influenced by the solar radiation as presented, where, in particular the power has been remarkably increased as shown in the figures 12 and 12.

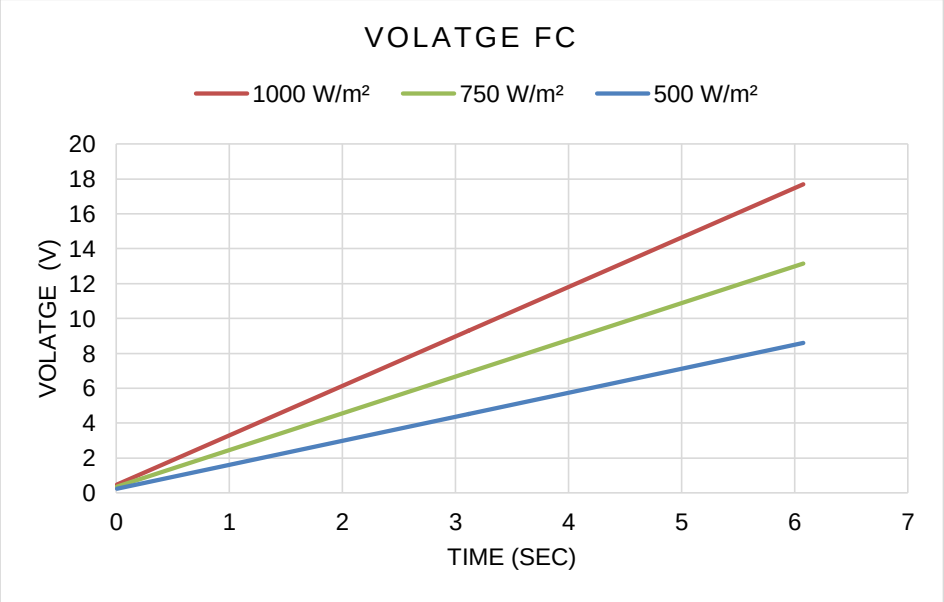

Figure 9: Fuel Cell voltage at various solar radiations and 50/50, PV and FC

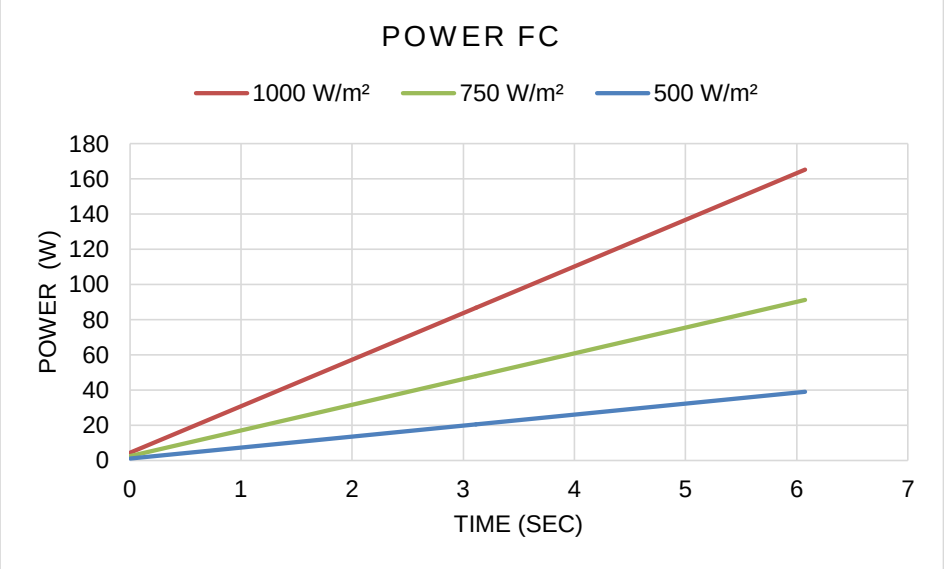

Figure 10: Fuel Cell Power at various solar radiations and 50/50, PV and FC

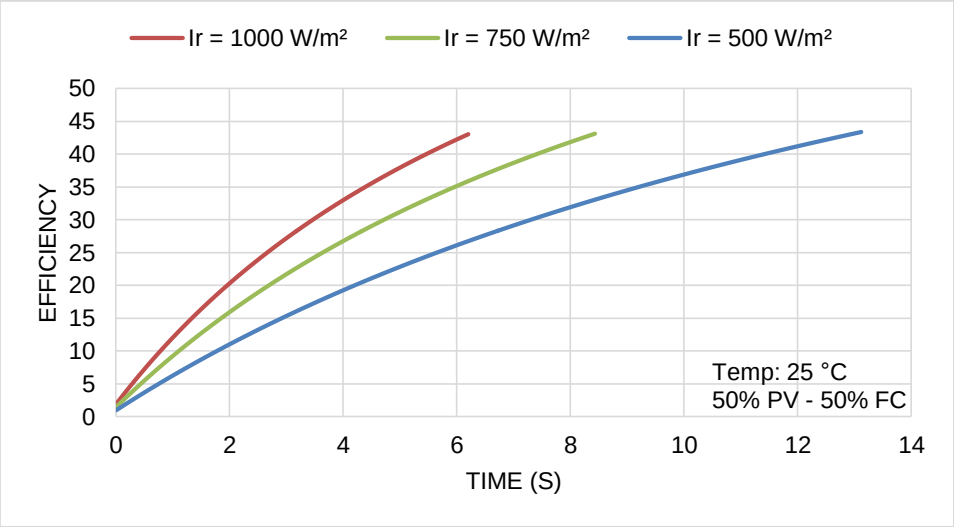

Figure 11: Fuel Cell Efficiency at various solar radiations and 50/50, PV and FC

Obviously, it can be concluded from these figures that the higher the solar radiation the higher the power produced by the fuel cell. However, as presented in these figures, the increase in solar radiations has similar impact on the transient behavior of the voltage and the fuel cell efficiency.

Furthermore, Figure 12 shows the Fuel Cell power at various voltage and solar radiations. It appears from the results presented in this figure that higher power can be produced at lower solar radiation and higher voltage.

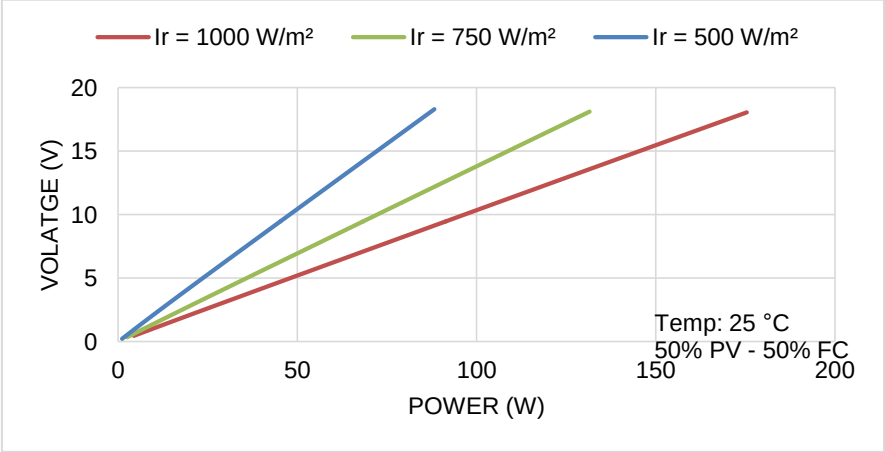

Figure 12: Fuel Cell Voltage and power at various solar radiations and 50/50, PV and FC

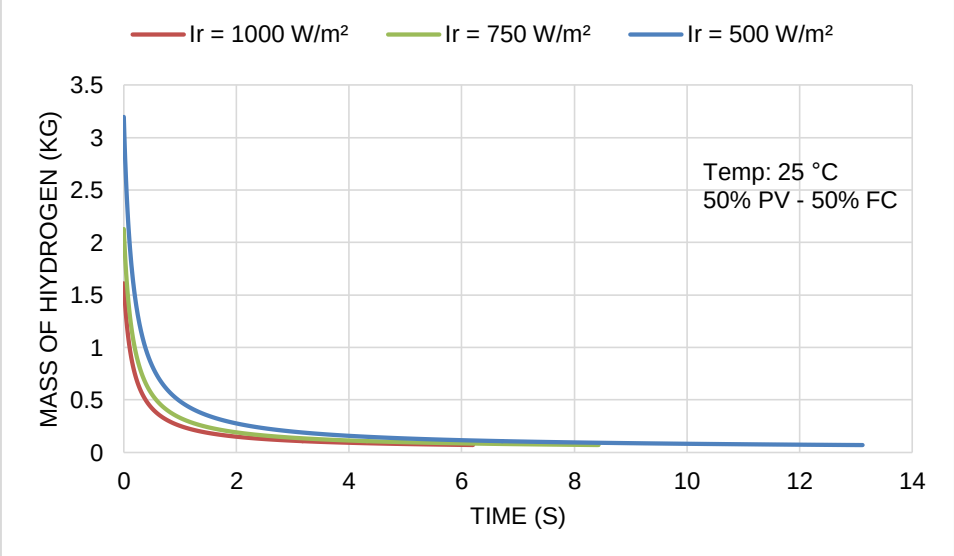

Figure 13: Fuel cell hydrogen mass at different solar radiations

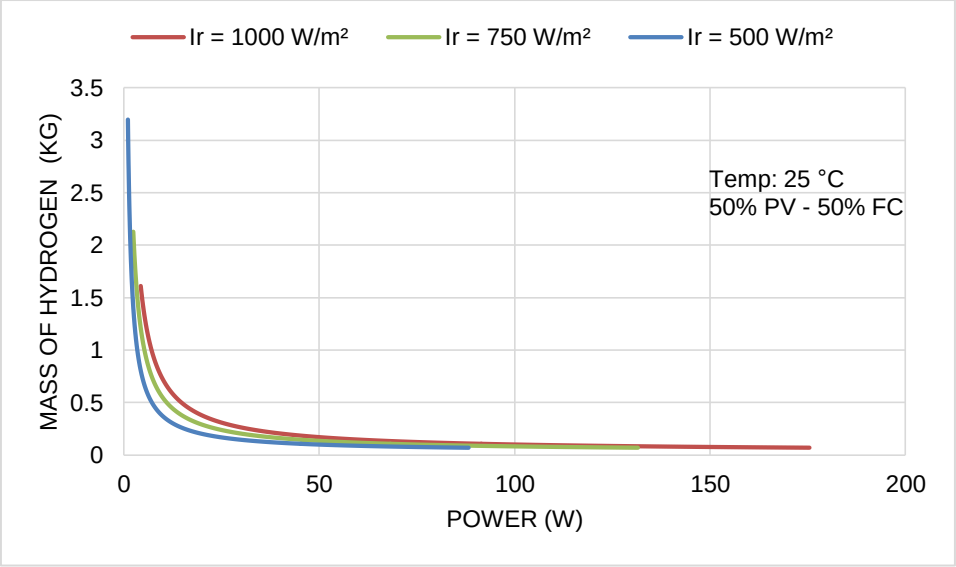

Figure 14: Fuel cell power and Hydrogen mass at different solar radiations

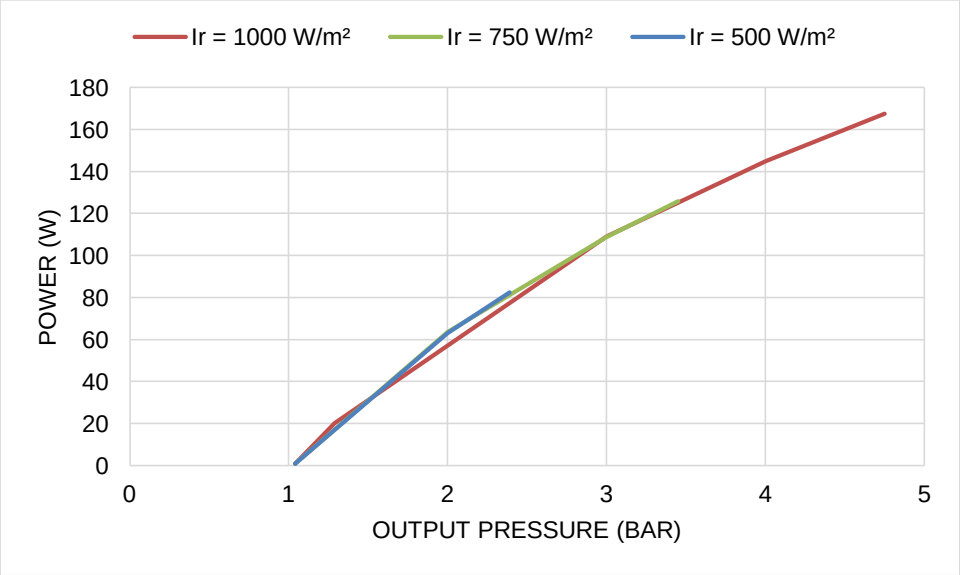

Figure 15: Fuel cell system compression power at different solar radiations

Figures 13 through 15 show the dynamic simulation results of the fuel cell in question predicted by the numerical model and in particular equations (13) through (19). The energy storage of hydrogen was calculated by equations (17) and (18) for different hydrogen mass and plotted at various solar radiations as well as other fuel cell parameters.

It is quite desirable to produce more fuel cell output with less hydrogen mass. Therefore, the storage capacity is reduced. The compressor energy needed to store the hydrogen mass is plotted in Figures 13 and 15 against the hydrogen mass for various compression pressure ratios, where it is assumed that the inlet pressure is 1 atm. It is obvious from equations (17) and (18) as well as the simulation results presented in Figure .15 that more energy compression is required at higher pressure ratios.

The simulated results of the fuel cell power and efficiency at various input power for various solar radiations are presented in the aforementioned figures. It is quite evident from the results in these figures that increasing the solar radiations will result in increasing fuel cell efficiency. To enhance the fuel cell efficiency, one must increase the load proportionally to the input power to drive the fuel cell which is consistent with what has been reported in the literature [10-20]. It is worthwhile mentioning that it was assumed in this simulation that 50% of the load is provided by the fuel cell based upon an electrolyzer efficiency of 50% and compression efficiency of 100%.

Hybrid System: Solar PV and PEM Fuel Cell:

In a hybrid photovoltaic–electrolyzer–PEM fuel cell system, the excess produced energy is stored as compressed hydrogen while the conversion is through the electrolyzer. The fuel cell is employed to generate power if the load exceeds what supplied by the solar Photovoltaic. In the study in question the load share is 50%/50% between the solar Photovoltiac and the fuel cell. The power output and

efficiency of the hybrid system in question including solar panels photovoltaic, electrolyzer, and hydrogen compression as well as fuel cell have been predicted for the hybrid by the aforementioned equations; (8) through (20) and presented in Figures. 16 through 18 as well as Figures 13 through 15.

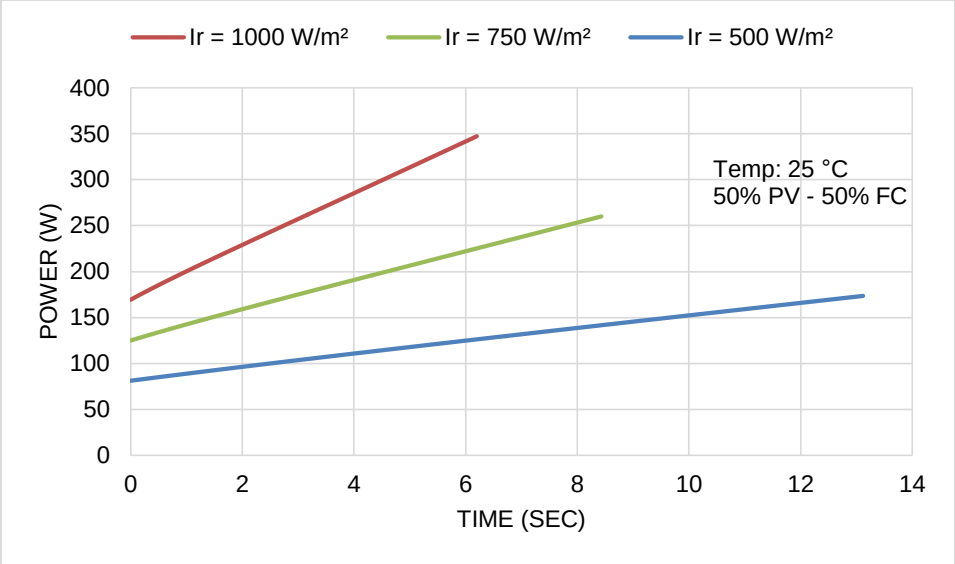

Figure 16: Hybrid system power at different solar radiations

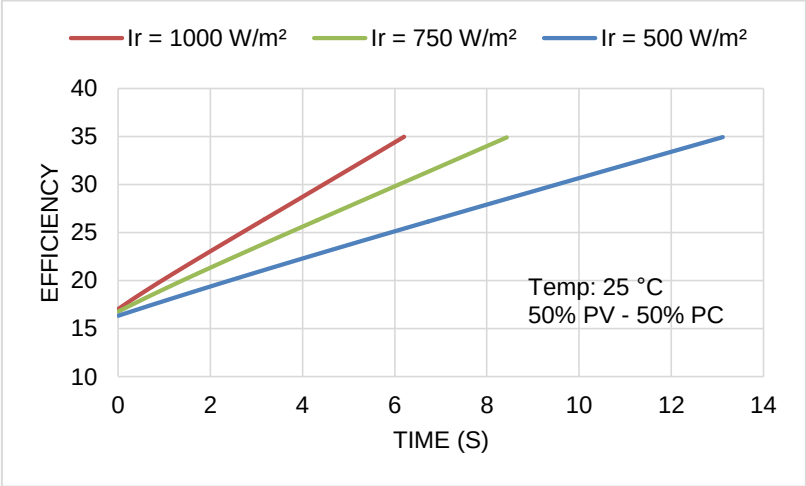

Figure 17: Hybrid system efficiency

It is quite clear from the results presented in the above-mentioned figures that the higher the fuel cell efficiency the maximum energy storage of hydrogen with small hydrogen mass. This consequently leads to higher fuel cell power output. The storage of hydrogen has significant value in supplying continuous power at periods of low solar irradiance. In addition, it can be used as a source of power and for electrification of remote areas that are disconnected from the grid.

As s shown in Figures. 1 and the simulated results in figures 16 and 17, the higher the solar radiation the higher the output power of the hybrid system which in turn enhances the hybrid system efficiency. Notably, figure 18 shows a typical power-efficiency characteristics of the hybrid system that illustrate the higher solar radiation results in higher output power of the hybrid system and higher hybrid system efficiency.

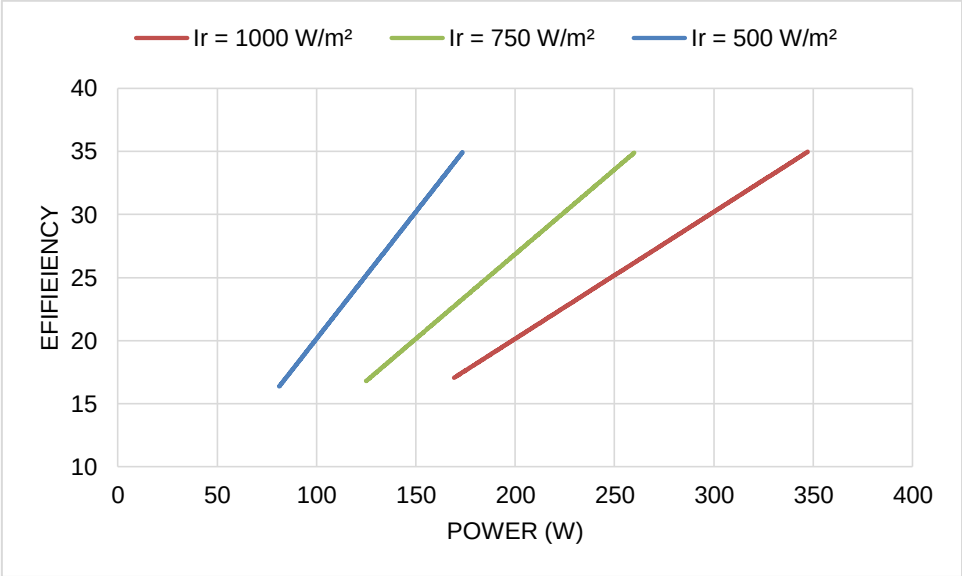

Figure 18: Hybrid system at different power and at different solar radiations

Simulation Model Validation:

In order to validate the prediction of our numerical model described in equations (1) through (27), we have used an experimental set up (C.F. 19) of the fuel cell described in the following;

- Basic PEM fuel cell model J101 with an area de 100 x 300 x 150 mm as shown in Figure.19
- An Electrolyzer with an area of 4 cm², with hydrogen production rate of 5 cm²/min and 2,5 cm²/min de oxygen.
- Two storage tanks for hydrogen and oxygen with capacity of 30 cm³ and distilled water.
- A fuel cell PEM H2 / O2 (PEM Fuel Cell H2 / O2) with an área of 4 cm², and power generation of e 500 mW, with voltaje from 0,4 to 0,96 V.
- A solar PV panel with an area of 90 cm², voltage 2 V, 350 mA at power .500 mW that drives electrolyzer PEM.

Comparisons between the predicted numerical values are presented in figures 20 through 27.

In particular, figures 20 through 23 showed that the simulated results predicted fairly of the PV cell temperature as well as other PV characteristics such as voltage, amperage, power and efficiency.

In an attempt to validate the numerical model prediction of the Fuel cell parameters, comparisons between the experimental Data and the mathematical model's prediction have been demonstrated in Figure. 24 through 26. Clearly the results presented in these figures show that the model predicted very well the data.

Figure 19: System Hybrid composed of fuel cell and solar PV setup

However, it is quite evident from the data presented in figure 24 that the numerical model predicted the data very well between output voltages up to 0.4 volts. It is in our opinion that the model over predicted the data of the voltage and the power as shown in Figures 24 and 25 because of the accuracy of the voltage and amperage sensors, and the

energy losses during the energy transfer between the electrolyzer and the fuel cell. It is also believed that the initial conditions and assumed parameters used in the simulation model contributed to the discrepancies.

Experimentally, the output power is calculated as the product of the amperage and voltage as plotted in the aforementioned figures. The efficiency values were calculated at the Fuel Cell experimental setup and was compared to that predicted by the model in question and plotted in Figure 26. It is quite evident that the efficiency was fairly predicted up to 20%. Values of hybrid system efficiency presented in figure 27 are in agreement with what has been reported in the literature.

Obviously, the hybrid system energy conversion efficiency will be affected by the solar irradiance among other parameters as shown in the previous figures. The dynamic results presented in Figure. 27 are consistent with others reported in the literature namely references [18, 20, 21, 28]. It has been observed from this figure that the model over predicted the dynamic efficiency of the hybrid system which is due to the issues previously explained.

As discussed in the aforementioned sections, in order to enhance the hybrid system efficiency, the load has to be increased promotionally with the increase of the solar irradiance. In other words, the hybrid system must be designed to match the load in order to operate at higher efficiency.

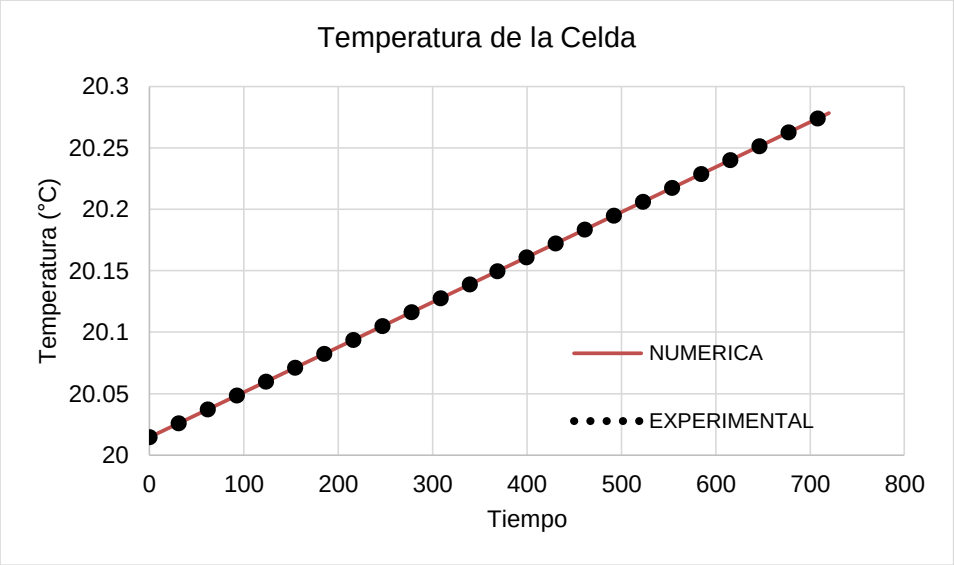

Figure 20: PV cell temperature at experimental setup

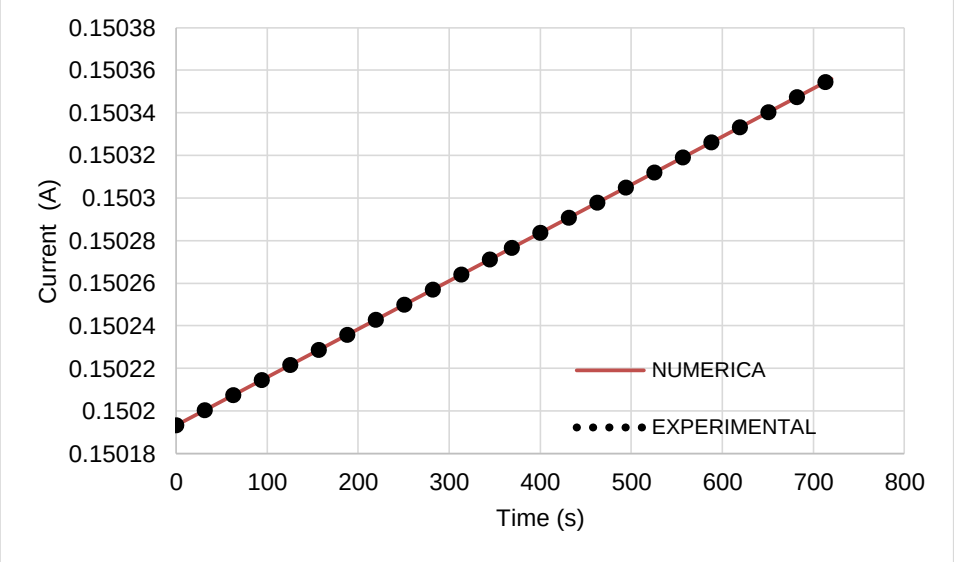

Figure 21: PV current at experimental setup

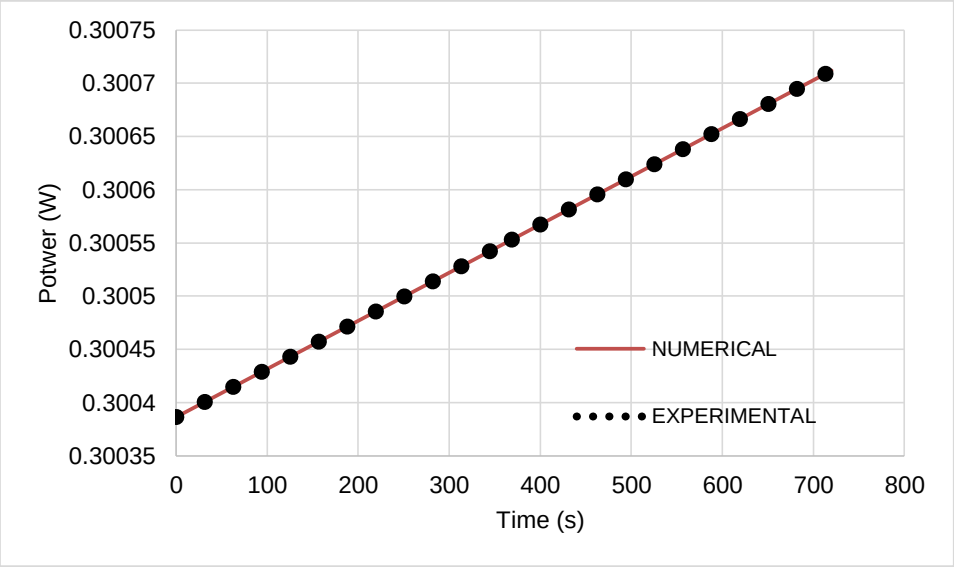

Figure 22: PV power at experimental setup

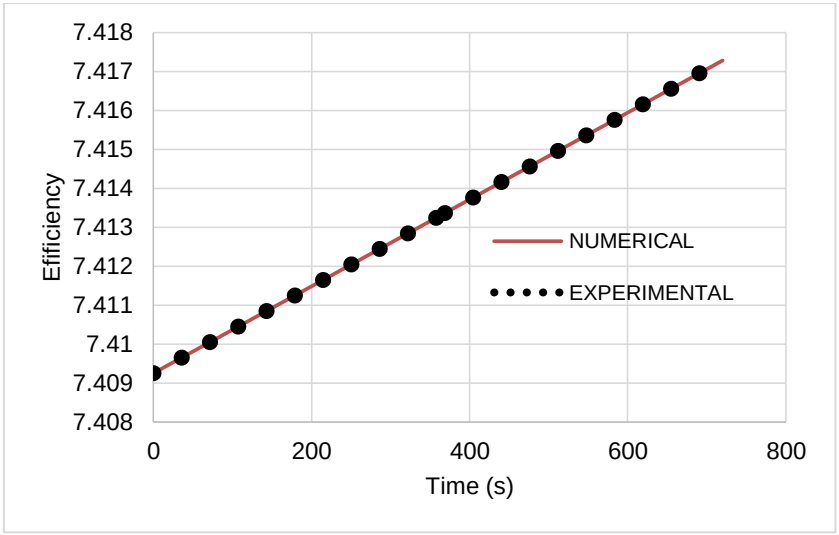

Figure 23: PV efficiency at experimental setup

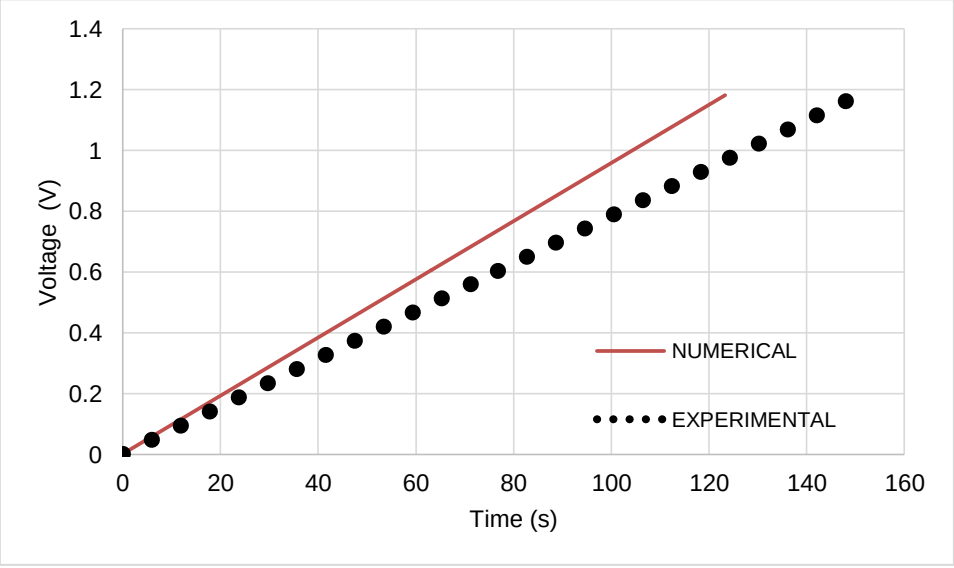

Figure 24. Voltage measured at Fuel Cell experimental setup

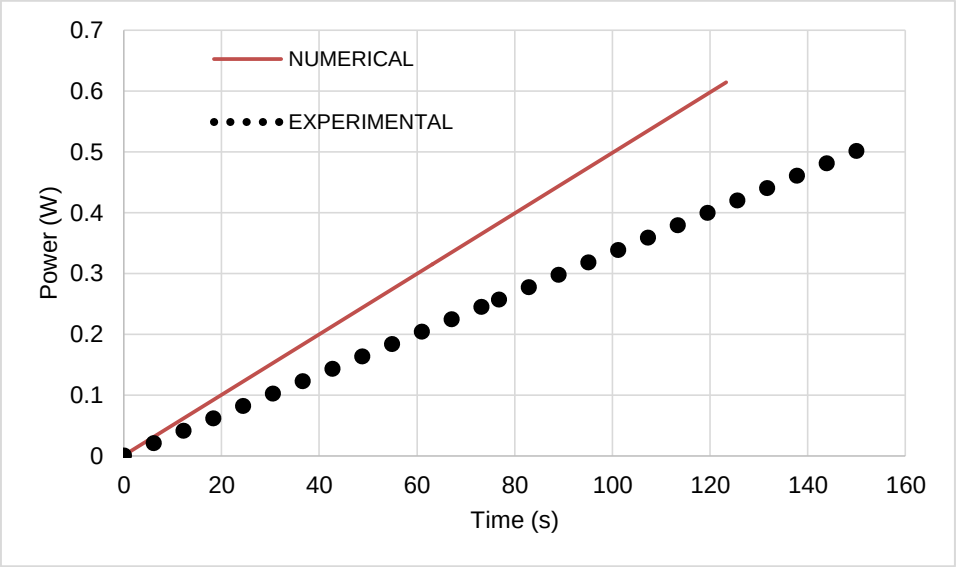

Figure 25. Power measured at Fuel Cell s experimental setup

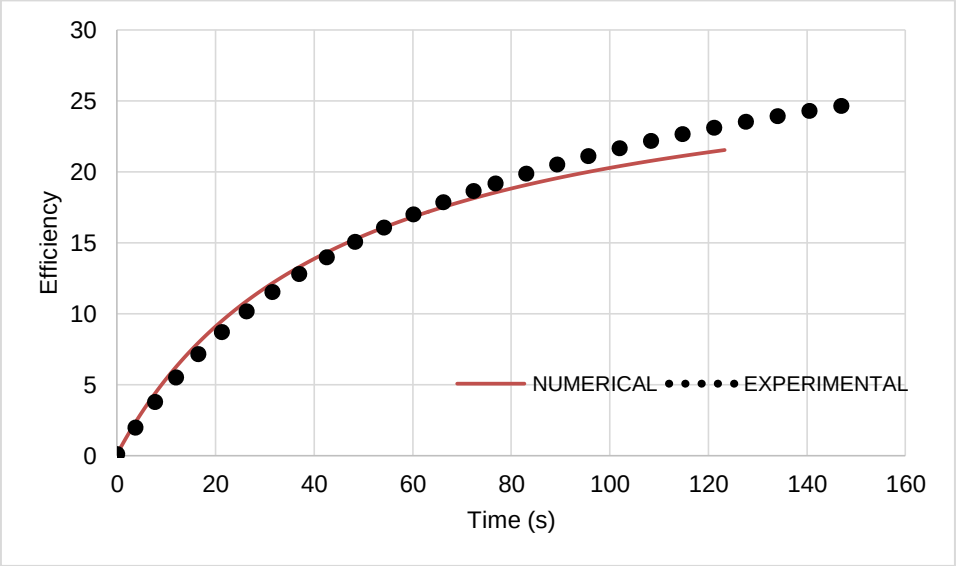

Figure 26. Efficiency predicted at Fuel Cell experimental setup

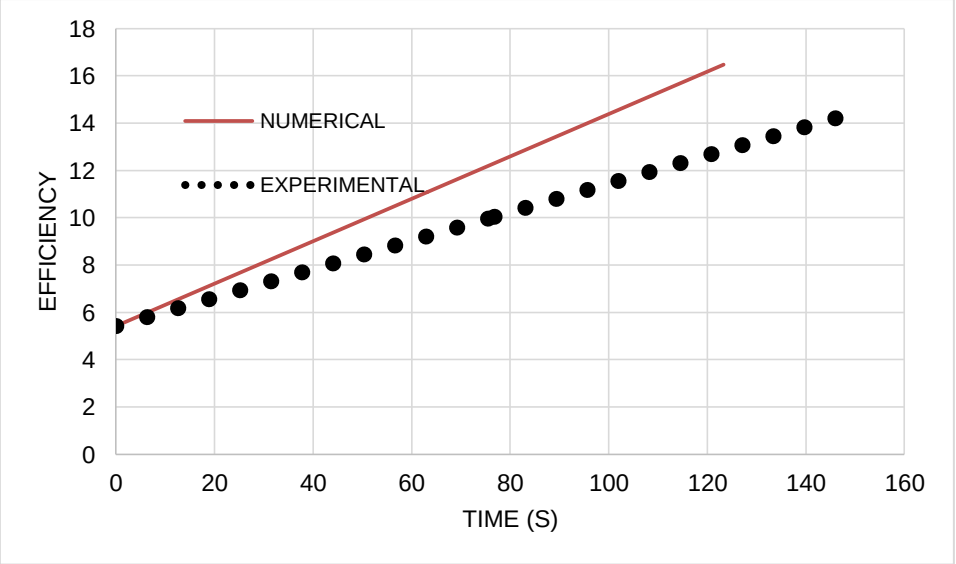

Figure 27. Hybrid system Efficiency calculated at PEM Experimental setup

Conclusions:

The energy conversion equations describing the total dynamic power generated and the key important parameters of a hybrid system of solar photovoltaic, and fuel cell PEM including hydrogen storage were presented, integrated simultaneously and analyzed. In addition, expressions for energy conversion efficiencies of each individual system as well as the hybrid system were also developed and presented. The different characteristics of the PV solar panel and fuel cell as well as the hybrid system were simulated at different conditions and different solar radiations. Comparison between the model predictions and the on-site data showed that the model fairly predicted the data under various conditions.

Nomenclature:

A_{pvg} = PV solar collector area (m^2)
$C_{compressor}$= Compressor energy
$E_{H2=}$ Hydrogen energy
G_t = Solar irradiation (W/m^2)
I_o= Single-phase current.
I_e= Current between electrodes.
I_{line}= Line current referred to wind turbine.
$I_{PV}(t)$= Current referred to PV in DC.
I_{rect}= DC current to the rectifier output.
J = Inertia moment of the generator [Kg-m^2].
K= Coefficient proportional to input kinetic energy.
K_1 = Constant of the inverter.
Kp= Coefficient of the controller.
LLP= Loss of load probability.
L_a= Inductance of armature [H].
M_{H2}= Mass of hydrogen.
N_{SBat}= Number of batteries connected in series.
P= Pressure
P(t)= AC power of the inverter output.
P_{3f}= Three phase AC power of the wind turbine.
P_{WT} = Wind power sweep produced by the blades.
P_{pv}= Nominal Power PV.
$P_{PV}(t)$= Electrical power DC of PV.
$P_{Cont-dc}$= Power Controller.
P_{inv-ip} = Inverter input power.
P_{inv-op} = Inverter output power.
R= Gas constant
R_a= Resistance of armature [Ω].
T= Temperature.
T_c = The collector temperature.
$T_{c\,ref}$ = The collector reference temperature.
Td = Time derivative of the controller.
v = Wind velocity
$V_{PV}(t)$= Voltage referred to PV in DC.
V_{bat} = Nominal voltage DC in the battery.
V_{fn} = Phase- neutral voltage.
V_{stack}= Fuel cell Stack voltage
$X_{H=}$ Hydrogen production rate

Greek alphabet

β = Temperature coefficient ((0.004 – 0.006) per °C)
η_g= Generator machine efficiency.
η_{pvg} = PV solar collector efficiency.
η_{pc} = power conditioning efficiency
η_r = The reference module efficiency
η_{c2}= The efficiency of conversion to DC referred to PV
η_{acc} = The losses efficiency.
η_{inv}= Inverter efficiency.
η_{sistem}= Hybrid system efficiency.
ρ_{air}= Air density.

Subscripts:

Air – Air
acc – Accessories
bat – Battery
$Cont - dc$ Controller
$c2$ – Conversion to DC referred to PV
fn – Phase neutral
FC- Fuel cell
$inv - ip$ - Inverter input
$inv - op$ - Inverter output
mp – Multiplication box
p – Power
pc – Power conditioning
PV – Photo Voltaic
pvg – Irradiance PV
rect – Rectifier
$SBat$ – Batteries connected in series.
$total$ – Total
$3f$ – Three phase AC

Acknowledgement:

The research work presented in this paper was made possible through the support of the Catholic University of Cuenca.

References:

1. Department of Energy, *Potential benefits of distributed generation and rate related issues that may impede their expansion*, A Study Pursuant to Section 1817 of the Energy Policy Act of 2005" 2007.
2. Binayak, B., Shiva, R. P., Kyung-Tae L., Sung-Hoon A. Mathematical modeling of hybrid renewable energy System: a review on small hydro-solar-wind power generation, International Journal of Precision engineering and Manufacturing-green Technology, 2014; 1, (2), pp. 157-173.
3. Kavitha S, and Kamdi, S.Y. Solar hydro hybrid energy system simulation, International Journal of Soft Computing and Engineering (IJSCE), 2013; 2, (6), pp. 500-503.

4. Nema, P., Nema, R.K., and Rangnekar, S. A review current and future state of art development of hybrid system using wind and PV-solar: a review, Renewable and Sustainable Energy Reviews, 2009; (13), 8, 2096-2103.
5. Akikur, R.K., Saidur, R., Ping, H., Ullah, K.R. Comparative study of stand-alone and hybrid solar energy systems suitable for off-grid rural electrification: A review. Renewable and Sustainable Energy Reviews, 2013; 27, 738-752.
6. Bhandari, B. *Design and evaluation of tri-hybrid renewable system (THRES)*, Ph. D. Thesis 2014; Department of Mechanical & Aerospace Engineering, Seoul National University.
7. Mahalakshmi, M. and Latha, S. Modeling and simulation and sizing of photovoltaic /wind/fuel cell hybrid generation system. International Journal of Engineering Science and Technology, IJEST, 2012; 4, (5).
8. Maharia, V., k and Dalal, G. Hybrid PV/fuel cell system design and simulation, International Journal of Science and Research, IJSR, 2014; 3, (9).
9. Kumar, S. and Garg, V. Hybrid system of PV solar/wind & fuel cell, International Journal of Advanced Research in Electrical, Electronics Instrumentation Engineering, IJAREEIE, 2013; 2, (8).
10. Touanti, S, Belkaid, A., Benabid, R., Halbaoui, K and Chelali, M. Pre-feasibility design and simulation of hybrid PV/fuel cell energy system for application to desalination plants loads, 2012; Procedia Engineering, 33, 366-376.
11. X. Hieu Nguyen y M. Phuong Nguyen, «Mathematical modeling of photovoltaic cell/ module/arrays,» *Environmental Systems Research*, pp. 1-13, 2015.
12. Sami, S. and Marin, E. "Simulation of Solar Photovoltaic, Biomass Gas Turbine and District Heating Hybrid System", International Journal of Sustainable Energy and Environmental Research, IJSEER, Vol. 6, No. 1, p 9-26, 2017
13. Sami, S. and Rivera, J. "A Predictive Numerical Model for Analyzing Performance of Solar Photovoltaic, Geothermal Hybrid System for Electricity Generation and District Heating", Science Journal Energy Engineering, SJEE, Volume 5, Issue 1, p 13-30, 2017.
14. Saha, N.C., Acharjee, S., Mollah, M.A.S., Rahman, K.T., and Rafi, F. H. M. Modeling and performance analysis of a hybrid power system, Proc. of International Conference on Informatics Electronics & Vision (ICIEV) 2013; pp. 1-5.
15. Mustafa, E. Sizing and simulation of PV-wind hybrid power system", International Journal of Photoenergy, 2013; 2013, Article ID 217526, 10 pages, 2013.
16. Saib, S. and Gherbi, A. Modeling and simulation of hybrid systems (PV/wind/battery) connected to the grid, International Conference on Electrical Engineering and Automatic Control, 2013; Setif, 24-26 November.
17. Najafizadegan, H and Zarabadipour, H. Control of voltage in proton exchange membrane fuel cell using model reference control approach", International Journal of Electochemical Science, 2012; 7, pp.6752-6761.
18. A. E. M. M. M. &. E.-A. A. Aly, "Modelling and simulation of a photovoltaic fuel cell hybrid system", Ph D thesis, Faculty of Electrical Engineering, University of Kassel, Germany, 2005.
19. M. Khan y M. Iqbal, «Dynamic Modeling and Simulation of a Small Wind-Fuel Cell Hybrid Energy System,» de *The 28th Annual Conference of the Solar Energy*, Kingstin,Canada, 2003.
20. Lin, J-C, Kunz, H.R., Fenton, M.F. and Fenton, S.S, The fuel cell –an ideal chemical engineering undergraduate experiment, 2013; Proceeding of the 2003 American Society for Engineering Education Annual Conference & Exposition, session 2313.
21. El-Shatter, Th. F, Eskandar, M.N. and El-Hagary, M.T. Hybrid PV/fuel cell system design and simulation, Renewable Energy, 2002; 27, pp. 479-485.
22. Ikhsan, M., Purwadi, A., Hariyanto, H., Heryana, N. and Haroen, Y. Study of renewable energy sources capacity and loading using data logger for sizing of solar-wind hybrid power system, 2013; 4th International Conference on Electrical Engineering and Informatics (ICEEI).
23. Bosma B. and Kallio G. *Renewable -energy labs for an undergraduate energy-systems course*, 2009; American Society for Engineering Education.
24. S. Benghanem, M. S., and Alamri, S. N. Modeling of photovoltaic module and experimental determination of serial resistance" JTUSCI, 2008; August.
25. Ramon, A., Lopez, Maritz, A. and Angarita, G. Parametros comparatives de celulas fotoelectricas para generaciob de energia: implementacion de banco de pruebas usando DSP comparative parameters of solar cells for power generation: test stand implementation using DSP. Ingeniería Energética 2014; XXXV, (3/2014), 193- 201, Septiembre/Diciembre ISSN 1815 – 5901.
26. Feroldi, D. Serra, M., Riera, J. Performance improvement of a PEMFC system controlling the cathode outlet air flow", J. Power Sources, 2007; 169, (1), 205-212.

27. Sami, S. and Icaza, D., Numerical Modeling, Simulation and Validation of Hybrid Solar Photovoltaic, Wind turbine and Fuel Cell Power System, JTIRE, Journal of Technology Innovations in Renewable Energy, Volume 4, No 3, 2015.

28. M. M. SALEH, R. ALI y H. ZHANG, Simplified mathematical model of proton exchange membrane fuel cell based on horizon fuel cell stack, Journal of Modern Power Systems and Clean Energy, vol. Volume 4, pp. 668-679, 2016.